Ain Shams Engineering Journal (2016) 7, 143–158

Ain Shams University

Ain Shams Engineering Journal

www.elsevier.com/locate/asej
www.sciencedirect.com

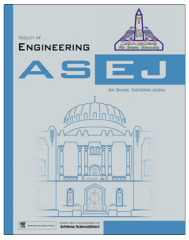

ELECTRICAL ENGINEERING

Performance comparison of TCSC with TCPS and SSSC controllers in AGC of realistic interconnected multi-source power system

Javad Morsali, Kazem Zare *, Mehrdad Tarafdar Hagh

Faculty of Electrical and Computer Engineering, University of Tabriz, Tabriz, Iran

Received 3 March 2015; revised 18 November 2015; accepted 27 November 2015
Available online 21 December 2015

KEYWORDS

AGC;
TCSC;
TCPS;
SSSC;
Realistic multi-source power system;
Frequency stability

Abstract The primary goals of employing series flexible ac transmission system (FACTS) in automatic generation control (AGC) studies of interconnected power systems are mitigating area frequency and tie-line power oscillations. This paper compares dynamic performance of thyristor controlled series capacitor (TCSC) as damping controller with thyristor controlled phase shifter (TCPS) and static synchronous series compensator (SSSC) which are series FACTS damping controllers. Commonly used lead-lag controllers are used in structure of damping controllers. The effect of TCSC in tie-line power exchange is modeled mathematically based on the Taylor series expansion for small-signal load disturbance. The performance of the proposed TCSC controller in coordination with integral AGC is compared with cases of TCPS–AGC and SSSC–AGC. An improved particle swarm optimization (IPSO) algorithm and integral of time multiplied squared error (ITSE) performance index are used to design the damping controllers. A two-area power system having generations from reheat thermal, hydro, and gas units in each area is evaluated regarding nonlinearity effects of generation rate constraint (GRC) and governor dead band (GDB). The simulations results in MATLAB/SIMULINK environment show that the proposed TCSC–AGC yields superior performance than others in damping of area frequencies and tie-line oscillations. Furthermore, sensitivity analyses are performed to show greater robustness of TCSC–AGC.

1. Introduction

1.1. Review on AGC in the presence of FACTS

Employing series flexible ac transmission system (FACTS) devices in automatic generation control (AGC) problem of interconnected power systems is an effective technique to increase the damping of tie-line and area frequency oscillations. This matter is an interesting topic that has received

* Corresponding author. Tel./fax: +98 413 330 0829.
E-mail addresses: morsali@tabrizu.ac.ir (J. Morsali), kazem.zare@tabrizu.ac.ir (K. Zare), tarafdar@tabrizu.ac.ir (M. Tarafdar Hagh).
Peer review under responsibility of Ain Shams University.

ELSEVIER Production and hosting by Elsevier

http://dx.doi.org/10.1016/j.asej.2015.11.012

much attention in the literature. Various series FACTS controllers can be used in series with tie-line of interconnected power systems to regulate the power flow and damp the inter-area oscillations through proposing a complementary damping controller. As a result of fast dynamic responses, series FACTS controllers such as thyristor controlled phase shifter (TCPS) [1–5] and static synchronous series compensator (SSSC) [4,6,7] have been applied in interconnected power systems to mitigate the area frequency and tie-line power oscillations. In [1], the dynamic performance of TCPS and capacitive energy storage (CES) for AGC of a hydro-thermal generation area connected to a hydro-diesel power system is compared using evolutionary algorithms. In [2], AGC analysis of a two-area interconnected power system under open market scenario is investigated in the presence of TCPS considering fuzzy logic controllers. In [3], a coordinated design of TCPS and superconducting magnetic energy storage (SMES) is studied for AGC of a deregulated hydrothermal power system considering generation rate constraint (GRC) of hydro and non-reheat thermal units. Authors in [4] deal with the coordinated controllers of SMES–SMES, TCPS–SMES and SSSC–SMES to compare their dynamic performance in AGC of an interconnected hydro-hydro power system. In [5], load frequency control (LFC) of an interconnected realistic multi-source power system is investigated with and without of TCPS in the tie-line. An interesting issue that has received much attention in the recent literature is performing of comparative studies between different FACTS devices such as TCPS and SSSC to show the effectiveness and dynamic performance. In doing so, the dynamic performance of SSSC and TCPS based damping controllers is evaluated in [4,6,7] along a two-area hydro-thermal power system in terms of settling time and overshoot of area frequency tie line power oscillations. A comprehensive literature survey on various AGC issues in conventional and distributed generation (DG) based power systems has been addressed in [8]. Besides, new findings and explorations on AGC incorporating FACTS based devices and energy storages, wind-diesel and PV systems have been reviewed.

Thyristor controlled series capacitor (TCSC) is widely employed in realistic power systems as a high-performance and cost-effective series FACTS for fine and secured optimal power flow (OPF) control in transmission lines [9,10]. The series compensation by TCSC is one of the most economic ways to release the capacity of transmission lines to carry more active power [11,12]. The TCSC controller can be employed to reduce efficiently the sub-synchronous resonance (SSR) [11]. Moreover, a complementary power swing damping (PSD) controller can be applied to TCSC to increase the rotor angle stability of multi-machine power system [13]. The coordinated design of TCSC-based PSD controller and power system stabilizer (PSS) is performed abundantly in recent years to improve the small-signal stability of power systems [14–17]. For the sake of comparison, the SSSC is a voltage source converter based on the gate turn off (GTO) switches whereas the TCSC and TCPS are based on thyristor controlled switches. Hence, the SSSC is an expensive solution and its cost and complexity are much higher than the TCSC [18,19]. Since the capacitors are cheaper than GTOs, the TCSC is price-wise more competitive than the SSSC [20]. Furthermore, the TCSC has much higher practical background [18] in comparison with the more sophisticated and expensive SSSC which has no stand-alone in-service practical application [21].

Due to simple and fast design of the lead-lag controllers, power system applications still prefer to use these linear structures rather than other nonlinear controllers. To the best of authors' knowledge, literature survey reveals that few papers deal with studying AGC in the presence of TCSC [22–24]. It is possible to mitigate the area frequency and tie-line power oscillations by dynamic controlling of series impedance of the tie-line with variable reactance of TCSC. In [22], a TCSC is located in series with the tie-line of a two-area thermal-thermal system with GRC and time delay considerations. SMES units are placed in both areas in coordination with TCSC to enhance the system dynamic performance. An incremental model has been developed for TCSC in [22] which is similar to the method proposed in [23,24]. The simulation results are compared with the case of without TCSC–SMES and the case of only TCSC. In [25], the performance of several FACTS devices such as SSSC, TCSC, TCPS, and interline power flow controller (IPFC) is compared in the presence of two degree of freedom integral plus double derivative (2DOF-IDD) controller in AGC of multi-area reheat thermal system. Though the given references in [25] about modeling of TCPS, SSSC, and IPFC in AGC studies are useful, the given references about TCSC modeling in AGC problem is not suitable. Most recently in [26], a novel modeling and simulation method for application of TCSC in AGC problem is proposed and dynamic performance of the TCSC–AGC coordinated controller is compared with the case of just AGC to damp the tie-line and area frequency oscillations in an interconnected multi-source power system. In this paper, this coordinated controller is compared with series FACTS controllers of TCPS and SSSC.

1.2. Survey on realistic issues having considerable impacts on AGC performance

In order to obtain an accurate realization of AGC problem, it is necessary to consider the main essential requirements of power system such as physical constraints of generation rate constraint (GRC), governor dead-band (GDB), nonlinearities [27–30] and the variety of power generations in each control area [5,31–33]. In [5], LFC of a two-area multi-source power system that has reheat thermal, gas, and hydro units in each area with a TCPS in series with the tie-line is reported. In [31,34], a HVDC link is considered in parallel with existing AC tie-line to interconnect the two areas of the multi-source power system. In order to obtain a realistic insight of the AGC problem, essential physical constraints such as time delay and GRC have been taken into account in [34]. In [32,34], the AGC is designed in deregulated environment for a two-area multi-source power system. In [33], a new population based parameter free optimization algorithm is proposed and its performance is validated on a multi-source power system having thermal, hydro and gas generating units. However, the nonlinearity effect of GRC of thermal and hydro units and the deteriorating the effect of GDB in thermal unit are not considered in [31–33]. It is observed that investigating the dynamic performance of AGC without regarding these issues may not show realistic results [35]. Surprisingly, the above literature review reveals that no significant effort has been made to assess the dynamic performance of AGC in a realistic situation such as validating on an interconnected multi-source

power system having gas, reheat thermal and hydro units with GRC and GDB nonlinearities alltogether in the presence of series FACTS controllers.

1.3. Main contributions of paper

In this paper, the dynamic performance of TCSC–AGC coordinated controller is compared with the TCPS–AGC and SSSC–AGC to damp effectively the tie-line power and area frequency oscillations of an interconnected realistic multi-source power system. The integral gains of AGC and adjustable parameters of the series damping controllers are optimized by an improved particle swarm optimization (IPSO) algorithm. The main contributions of this paper can be listed as follows:

(a) Comparative study on evaluating the dynamic performance of TCSC controller with TCPS and SSSC, all in coordination with AGC.
(b) Analyzing the dynamic performance of coordinated controllers on a realistic interconnected multi-source power system which has gas, hydro, and reheat thermal units considering GRC and GDB nonlinearities.

2. Under study power system

2.1. Realistic interconnected multi-source power system

The case study is a two-area interconnected power system with reheat thermal, hydro, and gas generations in each control area. Fig. 1 depicts the transfer function model of planed realistic power system. The details of hydro, reheat thermal, and gas units are outlined in Fig. 1. The considered generating units are combined together to build a control area which is represented by an equivalent unit dynamics. The parameters of the multi-source system are described in [26] and can be found in [5].

The GDB is defined as the total magnitude of a sustained speed variation within which there is no change in valve position of the turbine. Following recent works [26,36,37], the Fourier coefficients of N_1 and N_2 in transfer function of backlash type GDB are $N_1 = 0.8$ and $N_2 = -0.2/\pi$, respectively.

Practically, the rate of real power change, which can be achieved by thermal and hydro units, has a maximum limit. So, the designed LFC for unconstrained generation rate may not be realistic. The GRC of 10% /min for the thermal units is considered for both raising and falling rates. For the hydro unit, typical GRC of 270%/min and 360%/min for raising and falling generation is considered, respectively [1,28–30,38,39].

2.2. Tie-line power flow exchange modeling considering TCSC in series with the tie-line

The realistic and precise design of the TCSC control scheme is important since it directly affects the simulation accuracy and the dynamic performance of proposed controller. In this work, the procedure of extracting incremental tie-line power flow model proposed in [26] is considered. When a TCSC is inserted in series with the tie-line, the power flow exchange between the areas can be expressed as [26]:

$$\Delta P_{12}(s) = \Delta P_{12}^{0}(s) + \Delta P_{TCSC}(s) \tag{1}$$

in which,

$$\Delta P_{12}^{0}(s) = \frac{2\pi T_{12}}{S}[\Delta F_1(s) - \Delta F_2(s)] \tag{2}$$

$$\Delta P_{TCSC} = \Delta K_C + \Delta K_C^2 + \Delta K_C^3 + \Delta K_C^4 + \Delta K_C^5 + \ldots \tag{3}$$

where ΔP_{12}^{0} denotes the tie-line power flow exchange without TCSC and ΔP_{TCSC} represents the effect of presence of TCSC on the tie-line power flow exchange. As it is clear in (3), the tie-line power flow exchange can be regulated by controlling the compensation ratio ΔK_C as follows:

$$\Delta K_C(s) = \frac{K_{TCSC}}{1 + ST_{TCSC}} \frac{1 + ST_1}{1 + ST_2} \frac{1 + ST_3}{1 + ST_4} \Delta Error(s) \tag{4}$$

The structure of proposed TCSC-based damping controller is shown in Fig. 2 where the frequency deviation in area 1 i.e., Δf_1 is used as the control signal for TCSC controlling. It should be noted that according to the design objectives, only the first five terms in (3) are used in Fig. 2. The accuracy of this approximation is high and enough to avoid unnecessary and excessive complexities of simulations. The signal of *u(1)* in Fig. 2 denotes the value of $\Delta K_C(s)$ signal. The proposed TCSC control strategy that is based on Taylor series expansion called Taylor polynomials, is analytical, simple to follow, easy to implement in MATLAB/Simulink environment, and flexible to change its order of approximation.

2.3. Model of tie-line power flow exchange considering TCPS in series with tie-line

The TCPS is placed in series with the tie-line near one area to change the relative voltage phase angle between the areas. With considering TCPS, the tie-line power flow exchange from area 1 to area 2 can be written as [1,2,4,5,38]:

$$\Delta P_{12}(s) = \Delta P_{12}^{0}(s) + \Delta P_{TCPS}(s) \tag{5}$$

$$\Delta P_{12}^{0}(s) = \frac{2\pi T_{12}}{S}[\Delta F_1(s) - \Delta F_2(s)] \tag{6}$$

$$\Delta P_{TCPS}(s) = T_{12}\Delta\phi(s) \tag{7}$$

where $\Delta P_{12}^{0}(s)$ indicates the tie-line power flow exchange without TCPS, and the $\Delta P_{TCPS}(s)$ represents the impact of the presence of TCPS on the tie-line power exchange. The tie-line power can be regulated by controlling phase shifter angle $\Delta\phi(s)$, which can be represented as follows:

$$\Delta\phi(s) = \frac{K_{TCPS}}{1 + ST_{TCPS}} \Delta Error(s) \tag{8}$$

where K_{TCPS} and T_{TCPS} are the gain and time constants of the TCPS. The frequency deviation in area 1 Δf_1 can be utilized as the control signal to the TCPS to control the phase angle and subsequently the tie-line power [1,2,38]. Fig. 3 shows the MATLAB/SIMULINK block model of the TCPS controller. Thus, the power flow can be regulated to damp the tie-line power oscillations and thereby improve the interconnected power system stability.

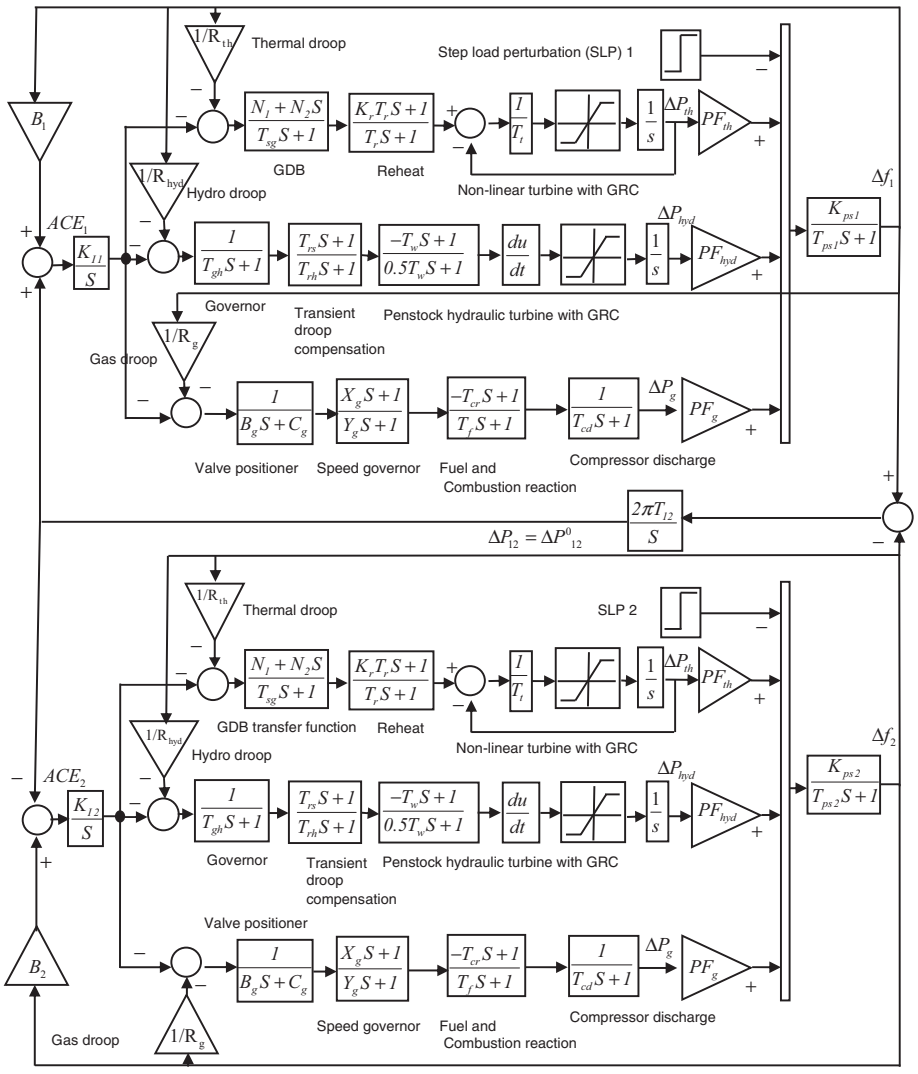

Figure 1 Transfer function model of proposed interconnected multi-source power system with GRC and GDB.

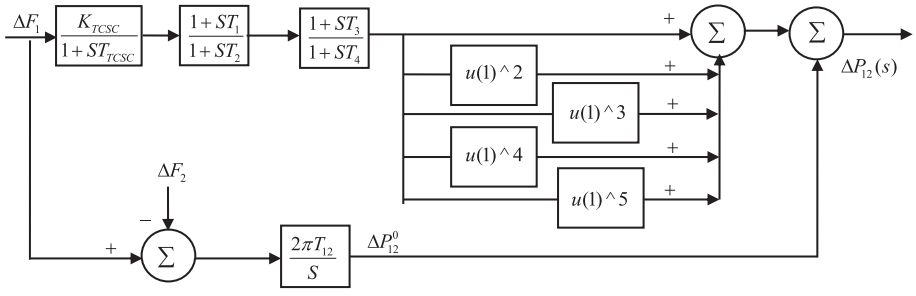

Figure 2 Structure of proposed TCSC as a frequency controller.

2.4. Model of tie-line power flow exchange considering SSSC in series with tie-line

The SSSC, placed in series with the tie-line between interconnected areas, can be employed to stabilize the area frequency and tie-line power oscillations by means of fast regulating the tie-line power flow. SSSC is represented by a series-connected voltage source in which the magnitude and polarity of injected voltage can be varied dynamically to imitate an inductive or a capacitive reactance affecting the power flow in transmission lines. Considering SSSC, the tie-line power flow exchange from area 1 to area 2 can be written as [4,6,7]:

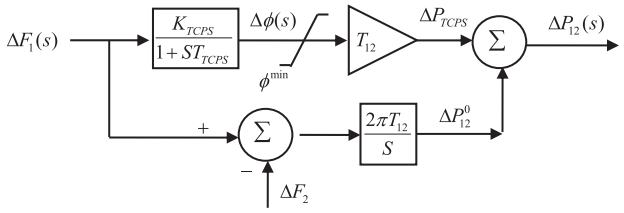

Figure 3 Modelling of TCPS as a frequency controller.

$$\Delta P_{12}(s) = \Delta P_{12}^0(s) + \Delta P_{SSSC}(s) \tag{9}$$

$$\Delta P_{12}^0(s) = \frac{2\pi T_{12}}{S}[\Delta F_1(s) - \Delta F_2(s)] \tag{10}$$

$$\Delta P_{SSSC}(s) = \frac{K_{SSSC}}{1+ST_{SSSC}} \frac{1+ST_1}{1+ST_2} \frac{1+ST_3}{1+ST_4} \Delta Error(s) \tag{11}$$

Fig. 4 shows block model of the SSSC controller in which the frequency deviation in area 1 is taken into account as input to the damping controller.

3. Problem formulation, simulation results and discussion

3.1. Objective function for controller design

In order to damp the tie-line power and frequency oscillations successfully, an appropriate objective function is essential to obtain the optimal controller parameters. In this work, the integral of time multiplied squared error (ITSE) performance index is regarded as the objective function which can be represented as follows:

$$ITSE = \int_0^{Tsim} t[\Delta f_1^2 + \Delta f_2^2 + \Delta P_{12}^2]dt \tag{12}$$

where T_{sim} denotes the simulation time. The ITSE index takes advantages of both integral of squared error (ISE) and integral of time multiplied absolute error (ITAE) performance indices, as it uses squared error and time multiplication to mitigate large oscillations and shorten long settling time. The ITSE performance index has been applied recently in [26,30,36,37] to design the optimal AGC of interconnected power systems. The adjustable parameters of coordinated controllers are summarized in Table 1. In both SSSC–AGC and TCSC–AGC controllers with lead-lag structure, the lead time constants (T_1, T_3) should be adjusted above the given values of corresponding lag time constants ($T_2 = T_4 = 0.01$ s) to fully compensate phase lag in the system.

A minimization problem is solved employing improved particle swarm optimization (IPSO) algorithm found in [26] to obtain the optimal parameters subject to following constraints:

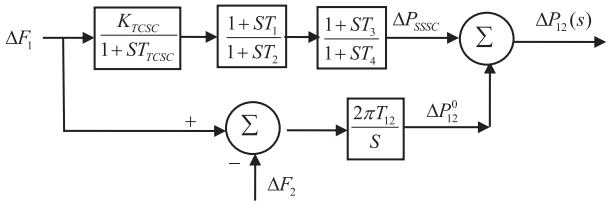

Figure 4 Modelling of SSSC as a frequency controller.

Table 1 Adjustable parameters of controllers.

Controller	Adjustable parameters
Integral controller (Just AGC)	K_{I1}, K_{I2}
TCSC–AGC coordinated controller	T_{TCSC}, K_{TCSC}, T_1, T_3, K_{I1}, K_{I2}
TCPS–AGC coordinated controller	T_{TCPS}, K_{TCPS}, K_{I1}, K_{I2}
SSSC–AGC coordinated controller	T_{SSSC}, K_{SSSC}, T_1, T_3, K_{I1}, K_{I2}

$$\begin{aligned}
&K_{I1}^{min} \leqslant K_{I1} \leqslant K_{I1}^{max}, K_{I2}^{min} \leqslant K_{I2} \leqslant K_{I2}^{max} \\
&K_{TCSC}^{min} \leqslant K_{TCSC} \leqslant K_{TCSC}^{max}, T_{TCSC}^{min} \leqslant T_{TCSC} \leqslant T_{TCSC}^{max}, \\
&T_1^{min} \leqslant T_1 \leqslant T_1^{max}, T_3^{min} \leqslant T_3 \leqslant T_3^{max} \\
&K_{TCPS}^{min} \leqslant K_{TCPS} \leqslant K_{TCPS}^{max}, T_{TCPS}^{min} \leqslant T_{TCPS} \leqslant T_{TCPS}^{max} \\
&K_{SSSC}^{min} \leqslant K_{SSSC} \leqslant K_{SSSC}^{max}, T_{SSSC}^{min} \leqslant T_{SSSC} \leqslant T_{SSSC}^{max}
\end{aligned} \tag{13}$$

where the gains and time constants are optimized in range of (0, 2) and (0.01, 1), respectively.

3.2. Simulation process

Before presenting the simulation outcomes, it seems to be useful to enumerate briefly what simulation procedure is going to carry out in continuation of this work to evaluate the performance of the controllers. The simulation process can be arranged as follows:

- Comparative performance evaluation of TCSC with SSSC and TCPS under step load perturbation (SLP) in area 1
- Performance comparison with various load perturbation patterns:
  1. Pulse load perturbation
  2. Sinusoidal load perturbation

- Sensitivity analysis to assess robustness of the controllers against ±50% uncertainty in system loading condition and parameters

3.3. Performance evaluation for SLP

In this case, the dynamic responses are obtained for 0.01 P.U. SLP in area 1 regarding the GRC and GDB nonlinearity effects. The objective is to minimize the ITSE index. The optimal parameters are listed in Table 2.

Fig. 5 illustrates the frequencies and tie-line power oscillation responses. It is notable to state that since the applied perturbation is an incremental load, the area frequencies drop down at first with undershoot. It can be observed from Fig. 5 that the AGC integral controller can difficultly return the deviations to zero with severe effort. As it is clear, even with the optimal AGC gains, the area frequencies and the tie-line power oscillations continue for a long time. Hence, the system with "Just AGC" can no longer restrain the frequency and tie-line power oscillations to return them to zero, effectively. It is explicit from Fig. 4 that the proposed TCSC–AGC damping controller outperforms the SSSC–AGC and TCPS–AGC in damping of area frequency and tie-line power oscillations.

Table 2 Optimal parameters of the controllers.

Controller	K_{I1}	K_{I2}	K_{FACTS}	T_{FACTS}	T_1	T_3
Just AGC [26]	0.0851	0.0457	–	–	–	–
TCSC–AGC [26]	0.1202	0.1800	0.1144	0.0599	0.5000	0.3108
SSSC–AGC	0.1100	0.4236	0.2795	0.8767	0.8921	0.9254
TCPS–AGC	0.0793	0.1154	1.2006	0.7976	–	–

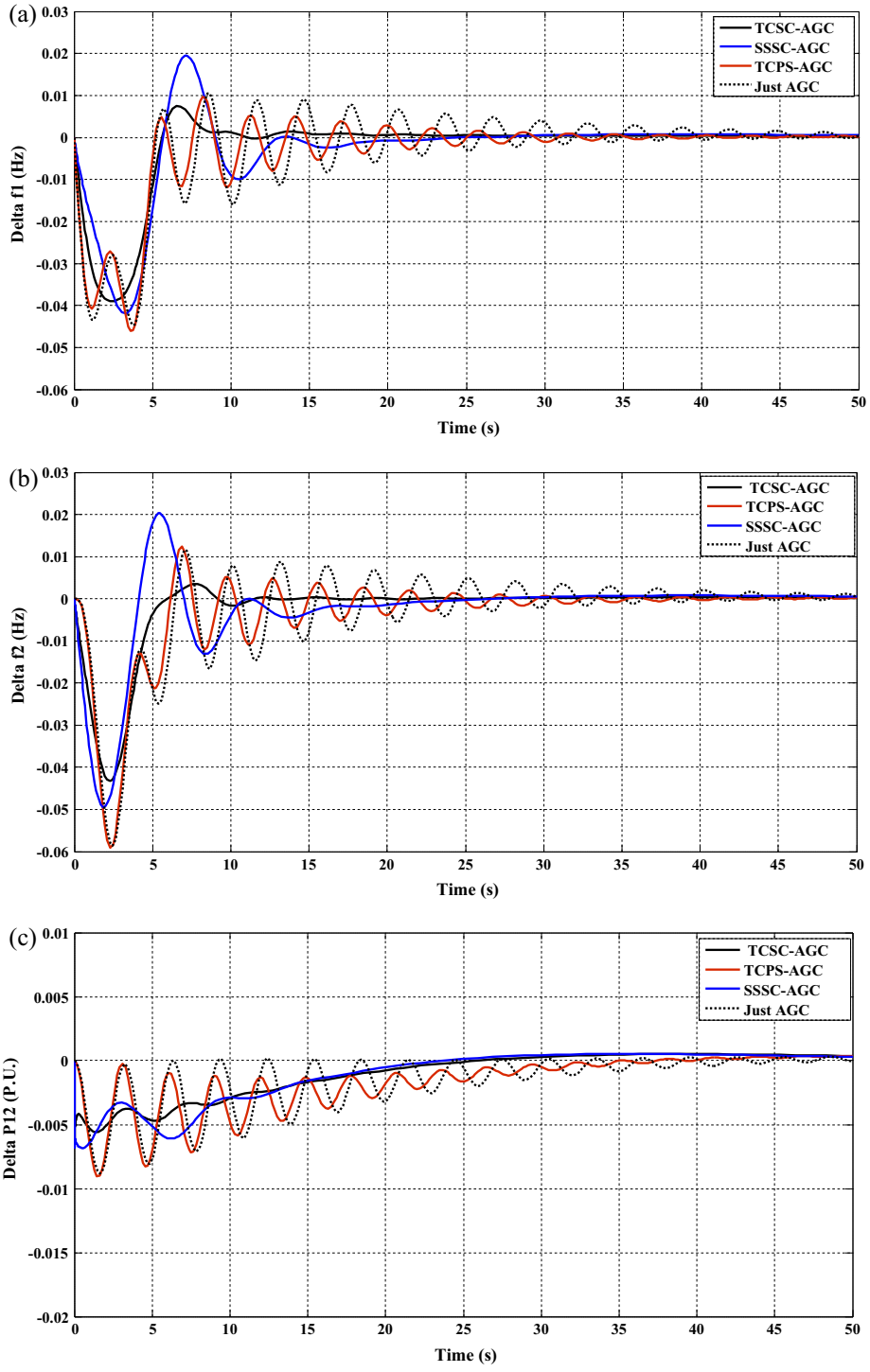

Figure 5 Dynamic responses to the SLP in area 1 using IPSO, (a) Area 1 frequency deviation, (b) Area 2 frequency deviation, and (c) Tie-line power deviation.

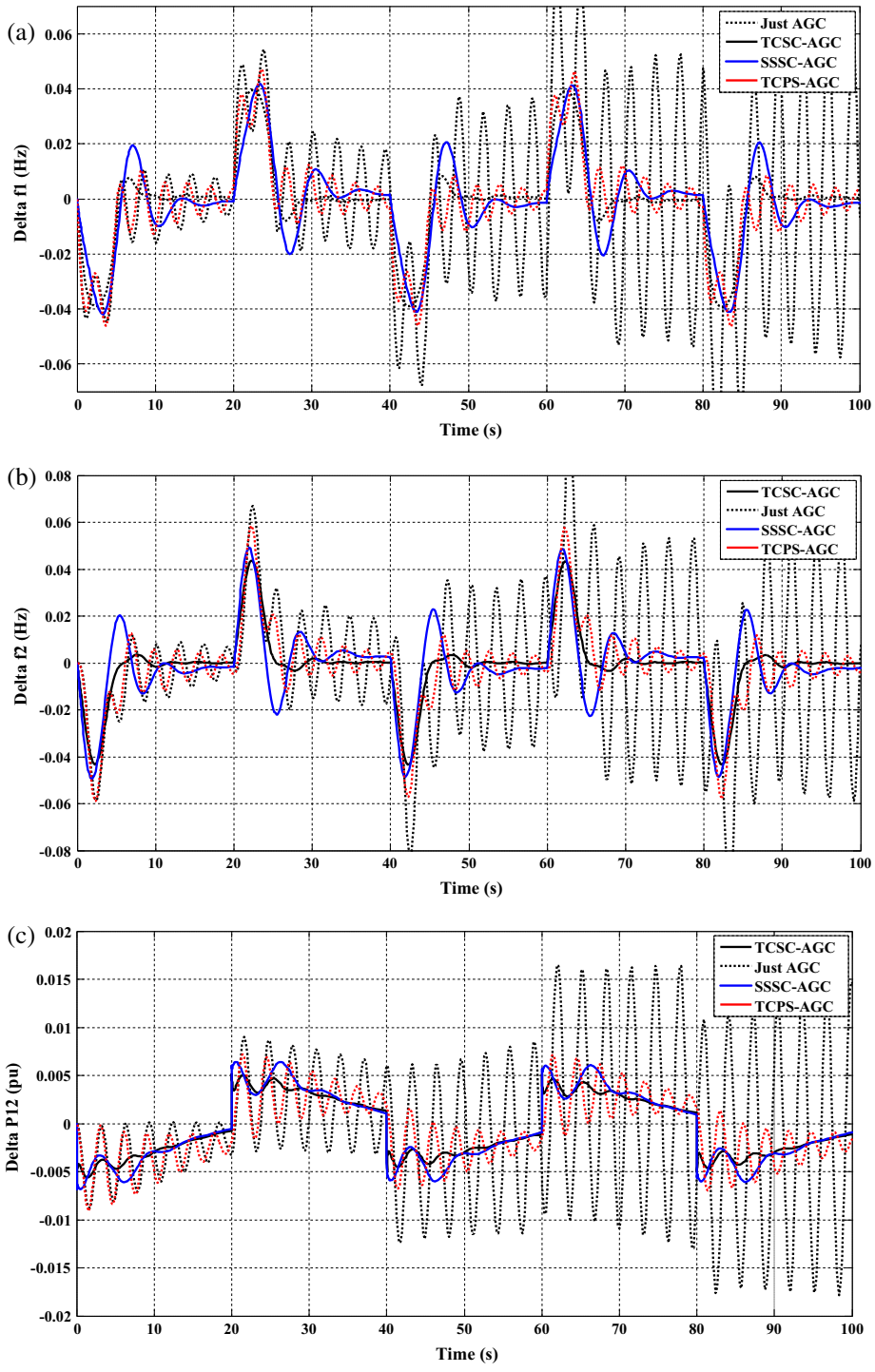

Figure 6 Dynamic responses to the pulse load perturbation in area 1: (a) Area 1 frequency deviation, (b) Area 2 frequency deviation, and (c) Tie-line power deviation.

The damping measures such as the value of ITSE index, maximum peak (M_p), peak time (T_P), and settling time (T_S) with 5% criterion, system oscillatory modes and damping ratios (ζ) with respect to the optimal controllers are reported in Table 3. These stability criteria are determinant in assessing AGC dynamic performance. Only the oscillatory modes obtained after linearization of the system are listed and the negative real eigenvalues are not listed here for simplicity. The linearization method obtains linear state space models from systems of differential equations described as Simulink models. The default algorithm uses pre-programmed analytic block Jacobians for the most blocks which should result in more accurate linearization than numerical perturbation of block inputs and states [40]. It is evident from Table 3 that

Table 3 System damping characteristics with the optimized controllers.

System oscillatory modes	ζ	f (Hz)	ITSE	Signal	M_p	T_P	T_S
Just AGC [26]							
−0.1711 ± 2.0357i	**0.0837**	0.3240	0.0621	Δf_1	0.0448	3.7452	48.4881
−0.6231 ± 0.5778i	0.7333	0.0920		Δf_2	0.0585	2.4691	50
−0.0695 ± 0.0251i	0.9407	0.0040		ΔP_{12}	0.0088	1.6309	38.2690
TCSC–AGC							
−103.9509 ± 136.0505i	**0.6071**	21.6531	0.0245	Δf_1	0.0390	2.4531	17.1614
−0.5424 ± 0.5565i	0.6979	0.0886		Δf_2	0.0432	2.2872	10.4525
−0.0691 ± 0.0599i	0.7555	0.0095		ΔP_{12}	0.0063	0.0226	21.1067
SSSC–AGC							
−99.6962 ± 125.4273i	0.6222	19.9624	0.0396	Δf_1	0.0420	3.3285	22.9392
−0.3710 ± 1.1509i	**0.3068**	0.1832		Δf_2	0.0494	1.8507	22.1176
−0.4742 ± 0.5752i	0.6361	0.0915		ΔP_{12}	0.0068	0.5051	25.3421
−0.0790 ± 0.0595i	0.7986	0.0095					
TCPS–AGC							
−0.2058 ± 2.1193i	**0.0967**	0.3373	0.0458	Δf_1	0.0461	3.6607	37.2932
−0.5935 ± 0.5698i	0.7213	0.0907		Δf_2	0.0588	2.2472	37.2932
−0.0629 ± 0.0403i	0.8417	0.0064		ΔP_{12}	0.0090	1.5008	30.4312

with proposed TCSC–AGC, the obtained ITSE index is the smallest value which means the most promising controller is this one. Furthermore, from Fig. 5 and Table 3, it is obvious that M_p, T_P, and T_S of the obtained responses by employing TCSC–AGC controller are remarkably smaller than those obtained by the SSSC–AGC and TCPS–AGC cases. Also, the system minimum damping ratio corresponding to the TCSC–AGC controller is at least two times of the others. If the eigenvalues are placed in the left hand side of the complex plain as much as is possible, the corresponding damping ratios grow larger and hence the overall system damping goes better. Briefly, the frequency stability is enhanced outstandingly by using the TCSC–AGC.

3.4. Performance evaluation for pulse load perturbation

In this item, a pulse load perturbation with period of 40 s and amplitude of 0.01 P.U. is applied in area 1. The area frequencies and tie-line power oscillation responses are shown in Fig. 6. It can be seen that by employing just AGC, the amplitude of the deviations grow larger consecutively which may bring about system instability. However, owing to the superiority of proposed TCSC–AGC controller in comparison with the SSSC–AGC and TCPS–AGC, the oscillations are mitigated appropriately even with the applied pulse perturbation.

3.5. Performance evaluation for sinusoidal load perturbation

In order to evaluate the effectiveness of considered controllers in stabilization of area frequencies and tie-line power oscillations under continuous load pattern, the sinusoidal load perturbation is applied in the area 1 as following [4]:

$$\Delta P_{d1} = 0.03\sin(4.36t) + 0.05\sin(5.3t) - 0.1\sin(6t) \quad (14)$$

Fig. 7 depicts the area 2 frequency and tie-line power oscillations under the sinusoidal load perturbation. The illustrations reveal that the oscillations are restricted effectively using the TCSC–AGC controller. As seen from Fig. 7, unlike to the previous perturbation patterns, only the amplitude of oscillations is limited which means that the oscillations are not damped out entirely due to the nature of the sinusoidal waveform. However, TCSC–AGC controller provides the greatest stabilizing performance to the oscillations in comparison with the SSSC–AGC and TCPS–AGC.

3.6. Sensitivity analysis against uncertainties

For robust analysis of the considered controllers against large uncertainties in the system loading condition and parameters, the sensitivity analysis is performed. Accordingly, the loading condition, governor time constant of thermal units T_{sg}, and the synchronizing coefficient T_{12} are deviated by ±50% of nominal values, independently. The results are presented in Table 4 for 0.01 P.U. SLP in area 1. It can be concluded from Table 4 that applying ±50% uncertainty in loading conditions, T_{sg}, and T_{12} leads to minor variations in ITSE index and other stability measures of the power system when it is equipped with the TCSC–AGC. In general, the value of ITSE index is related inversely to the system performance, i.e. the smaller the index shows the greater stability performance. The obtained illustrations under considered uncertainty scenarios are presented in Fig. 8. From the responses of depicted in Fig. 8, it can be observed that in the case of employing TCSC–AGC, the uncertainties have negligible impact on the system overall performance so, the frequencies and tie-line power deviations are restricted properly.

Briefly, the sensitivity analysis demonstrated that the system equipped with the adjusted TCSC–AGC controller is meaningfully insensitive one to the considered variations. As a result, once the adjustable parameters of TCSC–AGC controller are optimized in nominal condition, there is no need

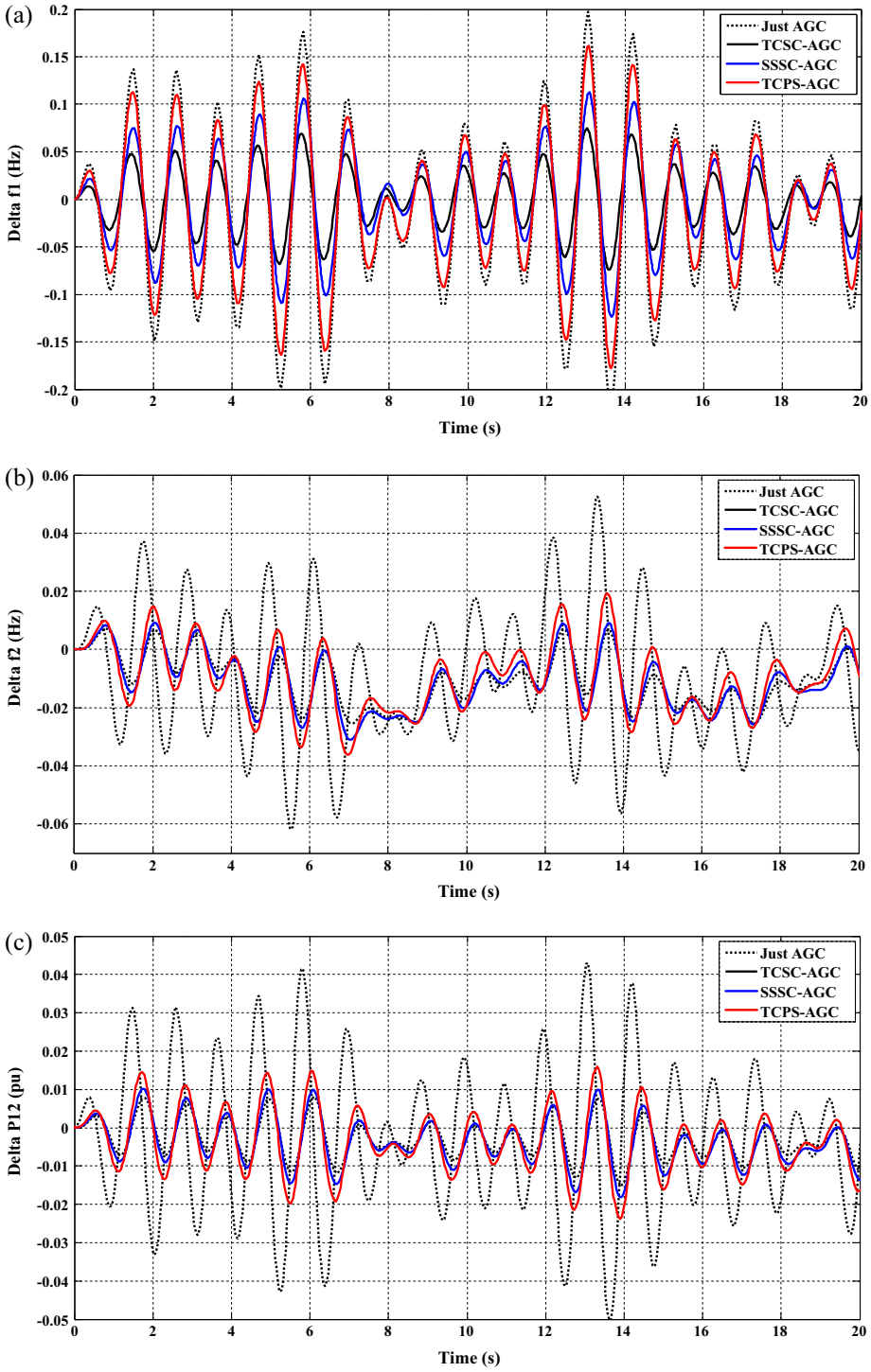

Figure 7 Dynamic responses to the sinusoidal load perturbation in area 1, (a) Area 1 frequency deviation, (b) Area 2 frequency deviation, and (c) Tie-line power deviation.

to reset for ±50% changes in the system parameters and loading condition.

3.7. IPSO versus standard PSO

PSO is a member of wide category of swarm intelligence-based optimization algorithms. The PSO is one of most well-known heuristic evolutionary algorithms which have found many applications in solving engineering optimization problems. The standard PSO has great advantages in comparison with similar swarm-based algorithms such as genetic algorithm (GA) [41]. The standard PSO has a few algorithm parameters while it uses a superior optimization technique to obtain the global optimal solution [41]. However, the standard PSO still may have some drawbacks such as exploration problem due to the risk of trapping in local minimal as a result of premature

Table 4 System dynamic performance with considered coordinated controllers under different uncertainties.

Uncertainty	% Change	Oscillatory modes	ζ	f (Hz)	ITSE	%Change	Signal	M_p
TCSC–AGC								
Loading condition	+50	−103.9644 ± 136.0605i	0.6071	21.6547	0.0211	−13.88	Δf_1	0.0372
		−0.5834 ± 0.5670i	0.7171	0.0902			Δf_2	0.0405
		−0.0691 ± 0.0598i	0.7558	0.0095			ΔP_{12}	0.0063
	−50	−103.9373 ± 136.0405i	0.6071	21.6515	0.0294	+20	Δf_1	0.0413
		−0.4994 ± 0.5463i	0.6747	0.0869			Δf_2	0.0461
		−0.0691 ± 0.0599i	0.7552	0.0095			ΔP_{12}	0.0063
T_{sg}	+50	−103.9497 ± 136.0511i	0.6071	21.6532	0.0250	+2.04	Δf_1	0.0392
		−0.5401 ± 0.5646i	0.6913	0.0899			Δf_2	0.0435
		−0.0690 ± 0.0600i	0.7547	0.0095			ΔP_{12}	0.0063
	−50	−103.9542 ± 136.0482i	0.6071	21.6527	0.0241	−1.63	Δf_1	0.0388
		−0.5441 ± 0.5488i	0.7041	0.0873			Δf_2	0.0429
		−0.0691 ± 0.0598i	0.7563	0.0095			ΔP_{12}	0.0063
T_{12}	+50	−103.9473 ± 136.0516i	0.6071	21.6533	0.0243	−0.82	Δf_1	0.0398
		−0.5409 ± 0.5557i	0.6975	0.0884			Δf_2	0.0433
		−0.0693 ± 0.0607i	0.7525	0.0097			ΔP_{12}	0.0063
	−50	−103.9544 ± 136.0495i	0.6071	21.6530	0.0255	+4.08	Δf_1	0.0399
		−0.5474 ± 0.5598i	0.6991	0.0891			Δf_2	0.0423
		−0.0684 ± 0.0575i	0.7654	0.0092			ΔP_{12}	0.0063
SSSC–AGC								
Loading condition	+50	−99.7095 ± 125.4379i	0.6223	19.9641	0.0317	−19.95	Δf_1	0.0394
		−0.3797 ± 1.1519i	0.3131	0.1833			Δf_2	0.0468
		−0.5169 ± 0.5699i	0.6718	0.0907			ΔP_{12}	0.0068
		−0.0787 ± 0.0593i	0.7990	0.0094				
	−50	−99.6829 ± 125.4166i	0.6222	19.9607	0.0519	+31.06	Δf_1	0.0448
		−0.3627 ± 1.1498i	0.3009	0.1830			Δf_2	0.0523
		−0.4324 ± 0.5819i	0.5965	0.0926			ΔP_{12}	0.0069
		−0.0792 ± 0.0598i	0.7981	0.0095				
T_{sg}	+50	−99.6949 ± 125.4279i	0.6222	19.9625	0.0409	+3.28	Δf_1	0.0422
		−0.3683 ± 1.1513i	0.3047	0.1832			Δf_2	0.0498
		−0.4735 ± 0.5832i	0.6303	0.0928			ΔP_{12}	0.0068
		−0.0790 ± 0.0597i	0.7978	0.0095				
	−50	−99.7000 ± 125.4248i	0.6223	19.9620	0.0382	−3.54	Δf_1	0.0416
		−0.3736 ± 1.1502i	0.3089	0.1831			Δf_2	0.0491
		−0.4745 ± 0.5675i	0.6415	0.0903			ΔP_{12}	0.0068
		−0.0790 ± 0.0594i	0.7993	0.0095				
T_{12}	+50	−99.6923 ± 125.4281i	0.6222	19.9625	0.0317	−19.95	Δf_1	0.0445
		−0.3877 ± 1.4110i	0.2650	0.2246			Δf_2	0.0463
		−0.4361 ± 0.5785i	0.6020	0.0921			ΔP_{12}	0.0068
		−0.0794 ± 0.0600i	0.7978	0.0095				
	−50	−99.7001 ± 125.4264i	0.6223	19.9622	0.0933	+135.61	Δf_1	0.0356
		−0.2990 ± 0.8598i	0.3284	0.1368			Δf_2	0.0537
		−0.6068 ± 0.5233i	0.7573	0.0833			ΔP_{12}	0.0070
		−0.0778 ± 0.0579i	0.8022	0.0092				
TCPS–AGC								
Loading condition	+50	−0.2302 ± 2.1203i	0.1079	0.3375	0.0356	−22.27	Δf_1	0.0422
		−0.6308 ± 0.5818i	0.7351	0.0926			Δf_2	0.0557
		−0.0629 ± 0.0403i	0.8421	0.0064			ΔP_{12}	0.0089
	−50	−0.1815 ± 2.1180i	0.0854	0.3371	0.0766	+67.25	Δf_1	0.0505
		−0.5549 ± 0.5569i	0.7058	0.0886			Δf_2	0.0622
		−0.0628 ± 0.0404i	0.8413	0.0064			ΔP_{12}	0.0092
T_{sg}	+50	−0.1957 ± 2.1234i	0.0918	0.3379	0.0486	+6.11	Δf_1	0.0463
		−0.5915 ± 0.5781i	0.7151	0.0920			Δf_2	0.0593
		−0.0628 ± 0.0404i	0.8410	0.0064			ΔP_{12}	0.0090
	−50	−0.2154 ± 2.1137i	0.1014	0.3364	0.0457	−0.22	Δf_1	0.0458
		−0.5949 ± 0.5618i	0.7270	0.0894			Δf_2	0.0589
		−0.0629 ± 0.0402i	0.8424	0.0064			ΔP_{12}	0.0090
T_{12}	+50	−0.1705 ± 2.5382i	0.0670	0.4040	0.0528	+15.28	Δf_1	0.0508
		−0.5935 ± 0.5698i	0.7213	0.0907			Δf_2	0.0559
		−0.0632 ± 0.0408i	0.8398	0.0065			ΔP_{12}	0.0094
	−50	−0.2656 ± 1.5698i	0.1668	0.2498	0.0415	−9.39	Δf_1	0.0521
		−0.5935 ± 0.5699i	0.7213	0.0907			Δf_2	0.0592
		−0.0620 ± 0.0388i	0.8475	0.0062			ΔP_{12}	0.0081

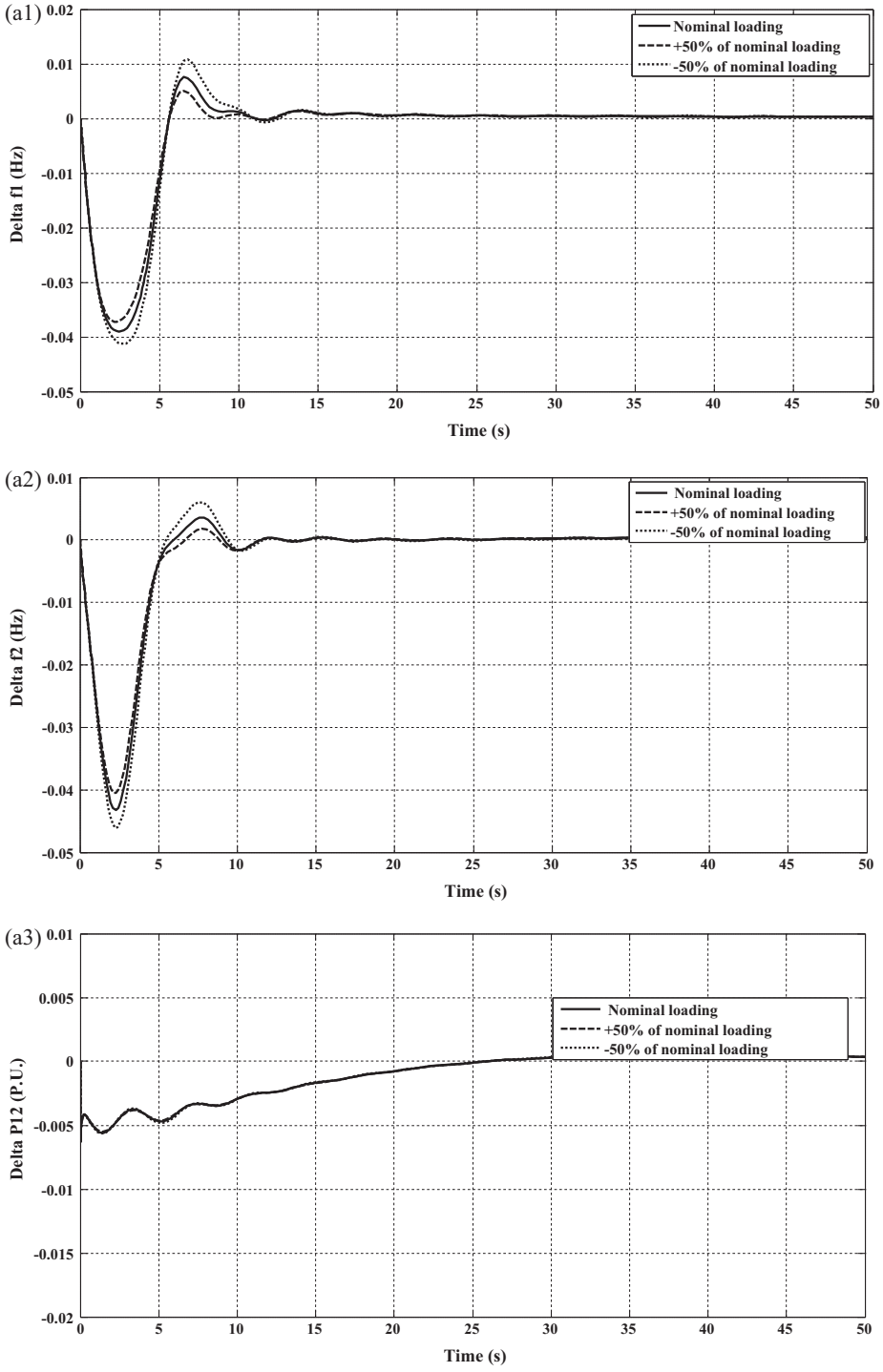

Figure 8 Dynamic responses of the system equipped with TCSC–AGC to the uncertainties in (a) loading condition, (b) T_{sg}, and (c) T_{12}.

convergence and exploitation problem due to inadequate capability to explore near borderline points of the search space [42]. In order to overcome the drawbacks of the standard PSO, an improved PSO (IPSO) algorithm has been introduced recently in [42]. This version of the PSO employs a new dynamic inertia weight by combining chaotic sequences with the linearly reducing inertia weights. Moreover, the IPSO uses a crossover operator inspired by the Genetic Algorithm (GA) to enhance both exploration and exploitation capabilities of the standard PSO. Thereby, the search quality is improved by avoiding premature convergence via increased diversity of the swarm. This can contribute in effective exploration and exploitation of the

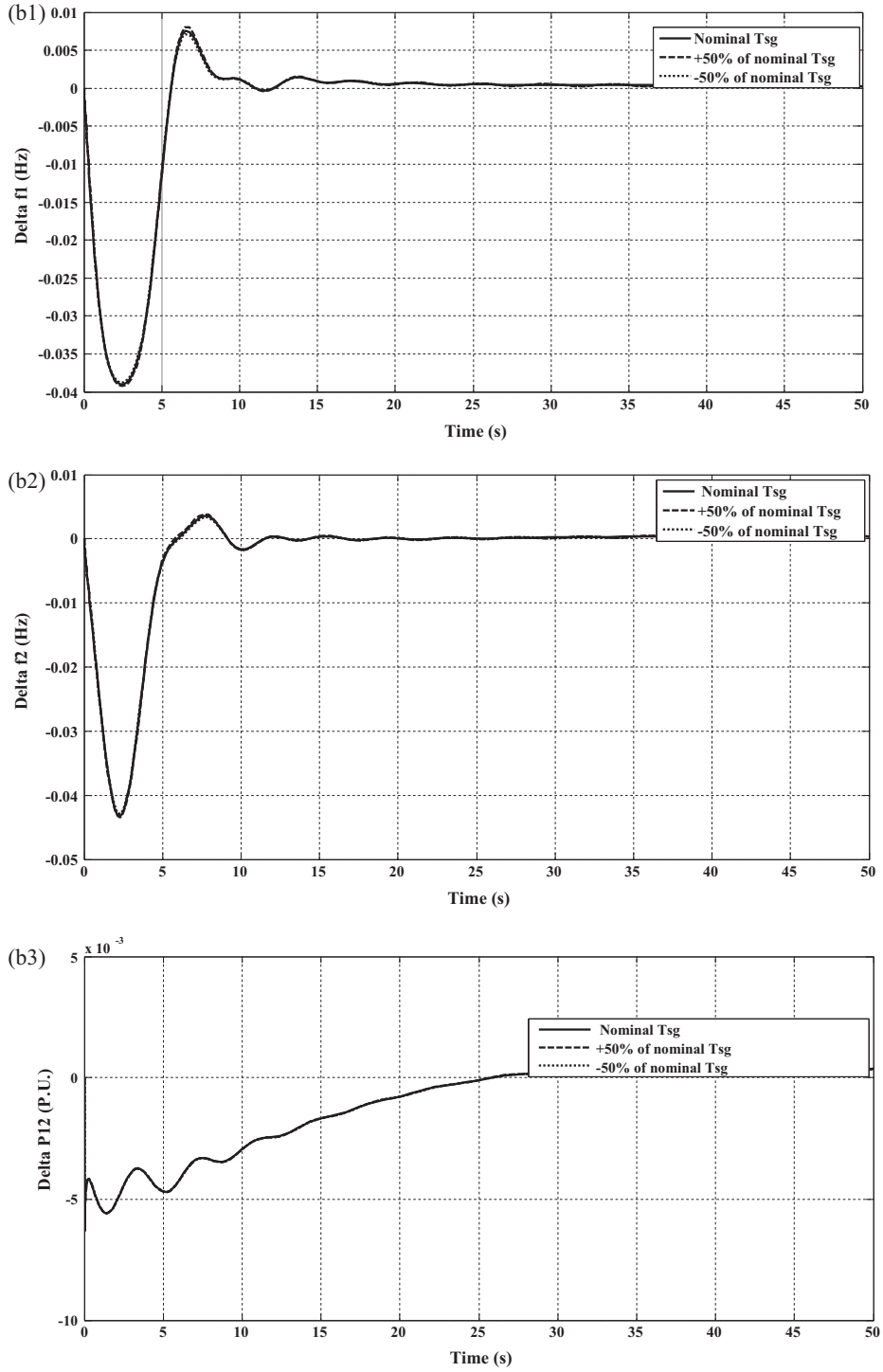

Figure 8 (*continued*)

favorable zones in the search space to find the global optimal solution more precisely. The parameters of the IPSO algorithm should be selected carefully to provide high performance. For our provided MATLAB-based IPSO program, the algorithm parameters are chosen as follows: $n = 30$; $m = 6$; $\omega_{min} = 0.4$; $\omega_{max} = 0.9$; $\mu = 4$; $\gamma_0 = 0.54$; $c_1 = c_2 = 2$; $\lambda = 0.1$; $iter_{max} = 30$; and CR = 0.6, where n is the population size; m is total number of parameters to be optimized; ω_{max}, ω_{min} are the initial and final inertia weights; μ is a control parameter; γ_0 is initial chaotic parameter; c_1, c_2 are acceleration coefficients; λ is a chosen number in interval (0, 1) to control the maximum velocity vector; $iter_{max}$ is the total number of the iterations; and CR is the crossover rate [42]. To compare the results, the standard PSO is also used to optimize the adjus-

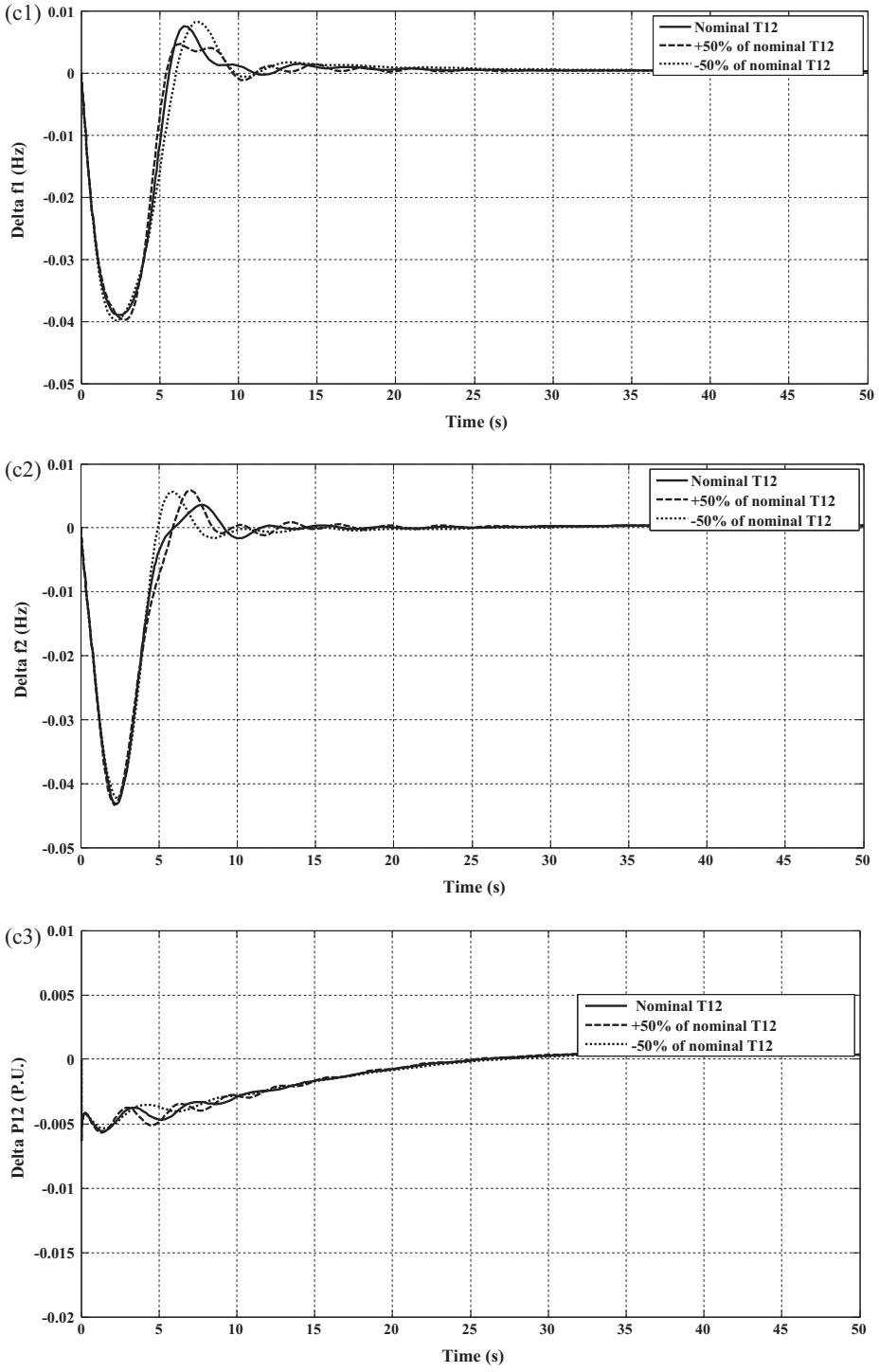

Figure 8 (*continued*)

table parameters of the TCSC–AGC coordinated controller. The parameters of the standard PSO are chosen as follows: $n = 30$; $m = 6$; $\omega_{min} = 0.4$; $\omega_{max} = 0.9$; $c_1 = c_2 = 2$; $\lambda = 0.1$; $iter_{max} = 30$. The optimized parameters obtained by the standard PSO are $K_{I1} = 0.1420$; $K_{I2} = 0.1980$; $K_{TCSC} = 0.0934$; $T_{TCSC} = 0.0621$; $T_1 = 0.4890$; $T_3 = 0.2054$; with ITSE = 0.0255. It can bee seen that by employing the standard PSO, the ITSE index is increased. Hence, the system overall performance is lower than that obtained by using the IPSO. Fig. 9 shows the frequencies and tie-line power oscillations for 0.01 P.U. SLP in the area 1. As it is obvious from Fig. 9, the oscillations are decreased more when the IPSO is used.

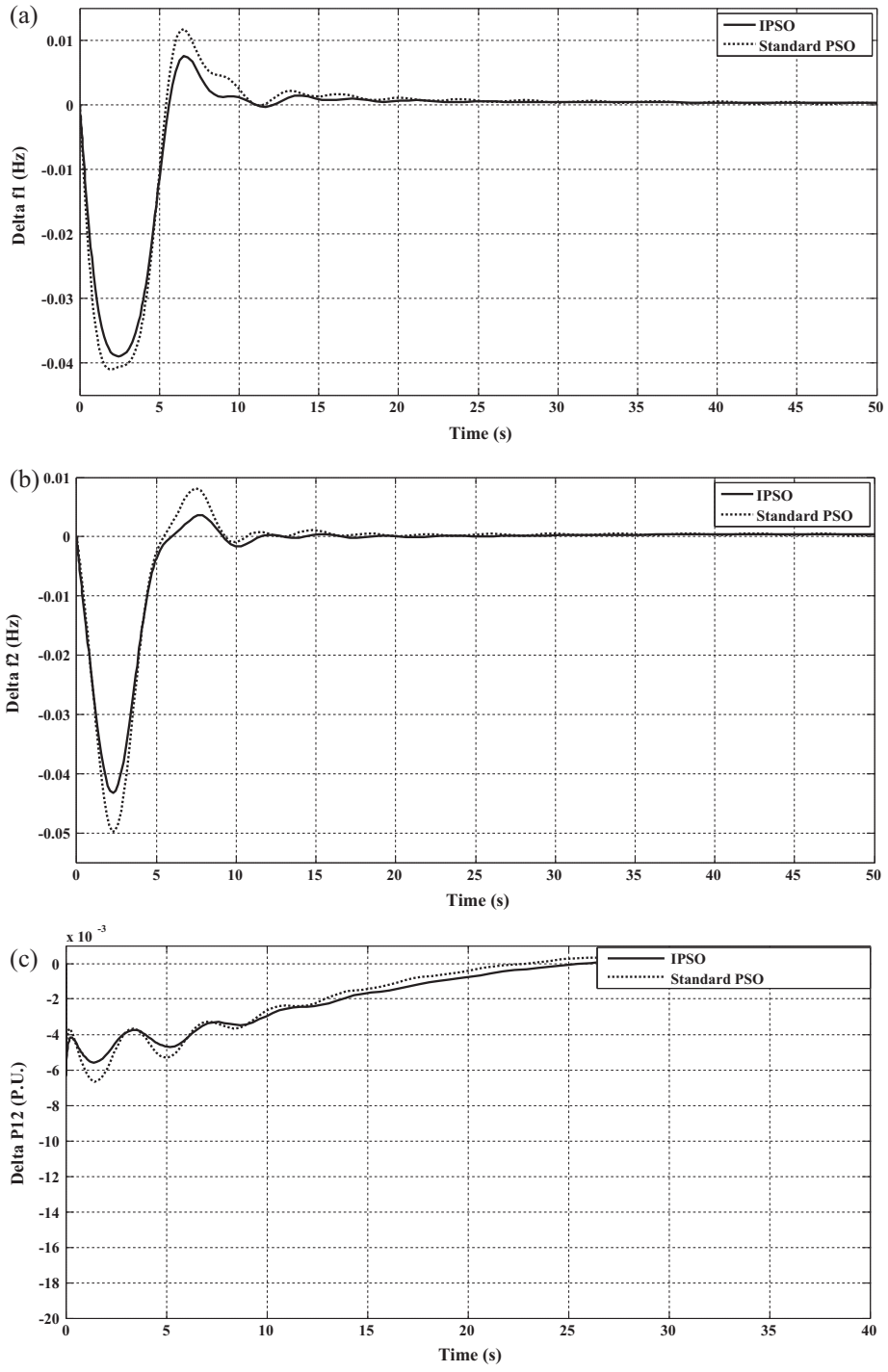

Figure 9 Dynamic responses with the TCSC–AGC using standard PSO algorithm, (a) Area 1 frequency deviation, (b) Area 2 frequency deviation, and (c) Tie-line power deviation.

4. Conclusion

In this work, an attempt has been made to compare the dynamic performance of novel coordinated controller (TCSC–AGC) with the existing SSSC–AGC and TCPS–AGC controllers. The Taylor series expansion is used in modeling of TCSC damping controller with well-known lead-lag structure. The obtained dynamic characteristics with considered coordinated controllers have been validated on the two-area realistic multi-source power system. The nonlinear time domain simulations for 0.1 P.U. SLP indicate that the TCSC–AGC controller provides the most superior dynamic performance in terms of decreased maximum peak, peak time, and settling time of area frequencies and tie-line power oscillations. Further performance evaluations are performed on the realistic interconnected multi-source power

system under pulse and sinusoidal load perturbation patterns. The sensitivity analyses with considering uncertainty scenarios in system loading condition and parameters demonstrate that the power system equipped with the optimized TCSC–AGC controller is quite insensitive to the variations in nominal conditions.

References

[1] Bhatt P, Roy R, Ghoshal S. GA/particle swarm intelligence based optimization of two specific varieties of controller devices applied to two-area multi-units automatic generation control. Int J Electr Power Energy Syst 2010;32(4):299–310.

[2] Rao CS, Nagaraju SS, Raju PS. Automatic generation control of TCPS based hydrothermal system under open market scenario: a fuzzy logic approach. Int J Electr Power Energy Syst 2009;31(7–8):315–22.

[3] Bhatt P, Ghoshal S, Roy R. Coordinated control of TCPS and SMES for frequency regulation of interconnected restructured power systems with dynamic participation from DFIG based wind farm. Renewable Energy 2012;40(1):40–50.

[4] Bhatt P, Roy R, Ghoshal S. Comparative performance evaluation of SMES–SMES, TCPS–SMES and SSSC–SMES controllers in automatic generation control for a two-area hydro–hydro system. Int J Electr Power Energy Syst 2011;33(10):1585–97.

[5] Parmar KPS, Majhi S, Kothari DP. LFC of an interconnected power system with thyristor controlled phase shifter in the tie line. Int J Comput Appl 2012;41(9):27–32.

[6] Subbaramaiah K. Comparison of performance of SSSC and TCPS in automatic generation control of hydrothermal system under deregulated scenario. Int J Electrical Comput Eng (IJECE) 2011;1(1):21–30.

[7] Darabian M, Jalilvand A. SSSC and TCPS based hydrothermal system to improve dynamic performance via FABFM. Int J Automation Power Eng (IJAPE) 2013;2(5):293–302.

[8] Pandey SK, Mohanty SR, Kishor N. A literature survey on load–frequency control for conventional and distribution generation power systems. Renew Sustain Energy Rev 2013;25:318–34.

[9] Meikandasivam S, Nema RK, Jain SK. Fine power flow control by split TCSC. Int J Electr Power Energy Syst 2013;45(1):519–29.

[10] Duong T, JianGang Y, Truong V. A new method for secured optimal power flow under normal and network contingencies via optimal location of TCSC. Int J Electr Power Energy Syst 2013;52:68–80.

[11] Mathur RM, Varma RK. Thyristor-based FACTS controllers for electrical transmission systems. John Wiley & Sons; 2002.

[12] Zhang X-P, Rehtanz C, Pal B. Flexible AC transmission systems: modelling and control. Springer; 2006.

[13] Ali E, Abd-Elazim S. TCSC damping controller design based on bacteria foraging optimization algorithm for a multimachine power system. Int J Electr Power Energy Syst 2012;37(1):23–30.

[14] Eslami M, Shareef H, Mohamed A, Khajehzadeh M. Gravitational search algorithm for coordinated design of PSS and TCSC as damping controller. J Central South Univ 2012;19(4):923–32.

[15] Morsali J, Kazemzadeh R, Azizian MR. Coordinated design of MPSS and TCSC-based damping controller using PSO to enhance multi-machine power system stability. In: Proceedings of the 21st Iranian conference on electrical engineering (ICEE2013), IEEE, Mashhad, Iran, 2013. p. 1–6.

[16] Morsali J, Kazemzadeh R, Azizian M, Parhizkar A. Introducing PID-based PSS2B stabilizer in coordination with TCSC damping controller to improve power system dynamic stability. In: Proceedings of the 22nd Iranian Conference on Electrical Engineering (ICEE2014), IEEE, Tehran, Iran, 2014. p. 836–41.

[17] Ali E, Abd-Elazim S. Coordinated design of PSSs and TCSC via bacterial swarm optimization algorithm in a multimachine power system. Int J Electr Power Energy Syst 2012;36(1):84–92.

[18] Ray S, Venayagamoorthy GK, Watanabe EH. A computational approach to optimal damping controller design for a GCSC. Power Delivery, IEEE Trans 2008;23(3):1673–81.

[19] de Jesus FD, Watanabe EH, de Souza LFW, Alves JER. SSR and power oscillation damping using gate-controlled series capacitors (GCSC). Power Delivery, IEEE Trans 2007;22(3):1806–12.

[20] Jowder F, Ooi B-T. Series compensation of radial power system by a combination of SSSC and dielectric capacitors. Power Delivery, IEEE Trans 2005;20(1):458–65.

[21] Jowder FA. Influence of mode of operation of the SSSC on the small disturbance and transient stability of a radial power system. Power Systems, IEEE Trans 2005;20(2):935–42.

[22] Padhan S, Sahu RK, Panda S. Automatic generation control with thyristor controlled series compensator including superconducting magnetic energy storage units. Ain Shams Eng J 2014;5(3):759–74.

[23] Abraham NM, Parameswaran AP, Abraham RJ. Effects of thyristor controlled series capacitor (TCSC) on oscillations in tie-line power and area frequencies in an interconnected non-reheat thermal power system. In: International conference on power and energy systems (ICPS), IEEE, Chennai, 22-24 Dec. 2011. p. 1–7.

[24] Saikia LC, Debbarma S, Sinha N, Dash P. AGC of a multi-area hydrothermal system using thyristor controlled series capacitor. In: Annual IEEE India Conference (INDICON), India, 2013.

[25] Dash P, Saikia LC, Sinha N. Comparison of performances of several FACTS devices using Cuckoo search algorithm optimized 2DOF controllers in multi-area AGC. Int J Electr Power Energy Syst 2015;65:316–24.

[26] Zare K, Hagh MT, Morsali J. Effective oscillation damping of an interconnected multi-source power system with automatic generation control and TCSC. Int J Electr Power Energy Syst 2015;65:220–30.

[27] Bernard MZ, Mohamed TH, Qudaih YS, Mitani Y. Decentralized load frequency control in an interconnected power system using coefficient diagram method. Int J Electr Power Energy Syst 2014;63:165–72.

[28] Velusami S, Chidambaram I. Decentralized biased dual mode controllers for load frequency control of interconnected power systems considering GDB and GRC non-linearities. Energy Convers Manage 2007;48(5):1691–702.

[29] Shiroei M, Toulabi MR, Ranjbar AM. Robust multivariable predictive based load frequency control considering generation rate constraint. Int J Electr Power Energy Syst 2013;46:405–13.

[30] Naidu K, Mokhlis H, Bakar A, Terzija V, Illias H. Application of firefly algorithm with online wavelet filter in automatic generation control of an interconnected reheat thermal power system. Int J Electr Power Energy Syst 2014;63:401–13.

[31] Mohanty B, Panda S, Hota P. Controller parameters tuning of differential evolution algorithm and its application to load frequency control of multi-source power system. Int J Electr Power Energy Syst 2014;54:77–85.

[32] Parmar K, Majhi S, Kothari D. LFC of an interconnected power system with multi-source power generation in deregulated power environment. Int J Electr Power Energy Syst 2014;57:277–86.

[33] Barisal A. Comparative performance analysis of teaching learning based optimization for automatic load frequency control of multi-source power systems. Int J Electr Power Energy Syst 2015;66:67–77.

[34] Sahu RK, Sekhar GC, Panda S. DE optimized fuzzy PID controller with derivative filter for LFC of multi source power system in deregulated environment. Ain Shams Eng J 2015;6(2):511–30.

[35] Bevrani H, Hiyama T. Intelligent automatic generation control. CRC Press; 2011.

[36] Sahu RK, Panda S, Rout UK. DE optimized parallel 2-DOF PID controller for load frequency control of power system with governor dead-band nonlinearity. Int J Electr Power Energy Syst 2013;49:19–33.

[37] Gozde H, Taplamacioglu MC. Automatic generation control application with craziness based particle swarm optimization in a thermal power system. Int J Electr Power Energy Syst 2011;33(1):8–16.
[38] Abraham RJ, Das D, Patra A. AGC study of a hydrothermal system with SMES and TCPS. Eur Trans Electrical Power 2009;19 (3):487–98.
[39] Parmar K, Majhi S, Kothari D. Load frequency control of a realistic power system with multi-source power generation. Int J Electr Power Energy Syst 2012;42(1):426–33.
[40] MathWorks, Inc. MATLAB: the language of technical computing. Desktop tools and development environment, version 7, MathWorks, 2005.
[41] Panigrahi BK, Abraham A, Das SE. Computational intelligence in power engineering. Berlin Heidelberg: Springer-Verlag; 2010.
[42] Park J-B, Jeong Y-W, Shin J-R, Lee KY. An improved particle swarm optimization for nonconvex economic dispatch problems. IEEE Trans Power Syst 2010;25(1):156–66.

Javad Morsali was born in Khoy, Iran, in 1986. He received his B.Sc. and M.Sc. degrees, both in electrical power engineering, from the University of Tabriz and Sahand University of Technology, Iran, in 2008 and 2011, respectively. He is the Ph.D. student in electrical power engineering at the University of Tabriz, since 2012. He has authored and co-authored more than 15 papers. His research interests include power system dynamics and stability, flexible ac transmission system (FACTS), automatic generation control (AGC), and power system deregulation.

Kazem Zare received the B.Sc. and M.Sc. degrees in Electrical Engineering from University of Tabriz, Tabriz, Iran in 2000 and 2003, respectively, and Ph.D. degree from Tarbiat Modares University, Tehran, Iran, in 2009. Currently, he is an Associate Professor of the Faculty of Electrical and Computer Engineering, University of Tabriz. His research areas include power system economics, distribution networks, microgrid, and energy management.

M. Tarafdar Hagh (S'98–M'06) received the B.Sc., M.Sc. (Hons.), and Ph.D. degrees in power engineering from the University of Tabriz, Tabriz, Iran, in 1989, 1992, and 2000, respectively. He has been with the Faculty of Electrical and Computer Engineering, University of Tabriz, since 2000, where he is currently a Professor. He has published more than 200 papers in power system and power-electronic-related topics. His interest topics include power system operation, distributed generation, flexible ac transmission systems, and power quality.